

COSMOLOGICAL CONSTANT OR INTERGALACTIC DUST? CONSTRAINTS FROM THE COSMIC FAR INFRARED BACKGROUND

ANTHONY AGUIRRE

Department of Astronomy, Harvard University
 60 Garden Street, Cambridge, MA 02138, USA
 email: aaguirre@cfa.harvard.edu

AND

ZOLTAN HAIMAN

NASA/Fermilab Astrophysics Center
 Fermi National Accelerator Laboratory, Batavia, IL 60510, USA
 email: zoltan@fnal.gov

Submitted to the Astrophysical Journal

ABSTRACT

Recent observations of Type Ia SNe at redshifts $0 < z < 1$ reveal a progressive dimming which has been interpreted as evidence for a cosmological constant of $\Omega_\Lambda \sim 0.7$. An alternative explanation of the SN results is an open universe with $\Omega_\Lambda = 0$ and the presence of $\gtrsim 0.1 \mu\text{m}$ dust grains with a mass density of $\Omega_{\text{dust}} \sim (\text{few}) \times 10^{-5}$ in the intergalactic (IG) medium. The same dust that dims the SNe absorbs the cosmic UV/optical background radiation around $\sim 1 \mu\text{m}$, and re-emits it at far infrared (FIR) wavelengths. Here we compare the FIR emission from IG dust with observations of the cosmic microwave (CMB) and cosmic far infrared backgrounds (FIRB) by the DIRBE/FIRAS instruments. We find that the emission would not lead to measurable distortion to the CMB, but would represent a substantial fraction ($\gtrsim 50\%$) of the measured value of the FIRB in the $300 - 1000 \mu\text{m}$ range. This contribution would be consistent with the present unresolved fraction of the observed FIRB in an open universe. However, we find that IG dust probably could not reconcile the standard $\Omega = 1$ CDM model with the SN observations, even if the necessary quantity of dust existed. Future observations able to resolve the FIRB to a flux limit of $\sim 0.5 \text{ mJy}$, along with a more precise measure of the coarse-grained FIRB, will provide a definitive test of the IG dust hypothesis in all cosmologies.

Subject headings: cosmology: theory – cosmology: observation – cosmology: Far Infrared Background – cosmic microwave background – galaxies: formation – galaxies: evolution

1. INTRODUCTION

One of the most remarkable results in recent observational cosmology is the detection of type Ia SNe at cosmological distances. Comparing the Hubble diagram of these ~ 50 SNe with the predictions of classical cosmological models strongly favors models with acceleration in the cosmic expansion, presumably due to a significant cosmological constant (Perlmutter et al. 1999; Riess et al. 1998). Given the far-reaching implications of this result, it is important to assess the possible systematic effects that could mimic the behavior of cosmic acceleration, and thus allow cosmologies without a cosmological constant.

Intergalactic (IG) dust could provide such a systematic effect. The amount of dust required to fully account for the systematic dimming of SNe at high redshift in an open universe is $\Omega_{\text{dust}} \sim (\text{few}) \times 10^{-5}$ (Aguirre 1999a; Aguirre 1999b [A99]). If this quantity of dust had the same composition as interstellar dust in the Milky Way, it would cause a significant reddening in the SN spectra, which is not observed. However, A99 showed that the removal of small dust grains during their ejection from galaxies into the IG medium could bias the composite dust cross section to cause little reddening for a given amount of extinction. A99 presented specific models for the evolution of the IG dust that are consistent with the observed lack of reddening, but provide the amount of extinction to fully account for the SNe results in an open universe.

In the present paper, we study the observational consequences of the IG dust hypothesis in far infrared wavelength bands. As is well known from previous studies, IG dust would efficiently absorb the UV/optical flux of galaxies and quasars, and re-radiate this energy in the far infrared (e.g. Wright 1981; Bond, Carr & Hogan 1991; Loeb & Haiman 1997). Although studied in great detail in these works, this effect is at present of renewed interest, owing to recent direct estimates of the global average comoving star formation rate (SFR) in the universe (e.g. Madau 1999 [M99]), and determinations of the extragalactic UV/optical background (UVB, Bernstein 1997), as well as of the cosmic far infrared background (FIRB, Fixsen et al. 1998). We thus have, for the first time, a measurement of both the UV reservoir available for dust absorption, as well as the background flux at the wavelengths where this energy would be emitted by the dust.

In this paper, we compute contributions to the FIRB and CMB arising from IG dust, and compare it to the measured values. Our aim is to assess whether the amount and type of dust that would explain the SNe results in an $\Omega_\Lambda = 0$ universe is compatible with these new observations.

At the present time, the source of the observed FIRB remains unclear. Deep observations with SCUBA have detected a population of discrete IR sources whose cumulative flux down in flux to $\sim 2 \text{ mJy}$ accounts for 20-30% of the FIRB at $850 \mu\text{m}$ (Barger et al. 1999a). The gravita-

tionally lensed sample of Blain et al. (1999) goes further down to ~ 1 mJy, but these authors detect only a single source fainter than ~ 2 mJy. It is not yet clear, then, whether the luminosity function of these objects continues to sufficiently faint fluxes to account for 100% of the FIRB. Furthermore, we lack information on the spectra of these sources at wavelengths other than $850 \mu\text{m}$. Although the full FIRB can be explained theoretically in semi-analytic galaxy formation models (Guiderdoni et al. 1998), this requires the somewhat ad-hoc postulate that the ratio of the number of ULIGs (a population of “ultraluminous infrared galaxies”) to that of normal optical galaxies increases rapidly with redshift. In summary, according to our present knowledge, a fraction 70-80% of the FIRB could still be contributed by diffuse emission from IG dust.

As in the case of the FIRB, the nature of the observed UVB is unclear. The directly observed values at 0.55 and $0.8 \mu\text{m}$ are $20 \pm 10 \text{ nW m}^{-2} \text{ sr}^{-1}$ (Bernstein 1997). By comparison, a recent compilation of ground based galaxy counts, and a survey of galaxies in the Hubble Deep Field (HDF) has yielded an estimate for the evolution of the global star formation rate in the universe between $0 < z \lesssim 5$. The UVB that follows from a census of these galaxies is around $\sim 12 \text{ nW m}^{-2} \text{ sr}^{-1}$ (Madau 1999 [M99]; Pozzetti et al. 1998), a factor of ~ 2 smaller than the observed value. A natural explanation for the difference would be if the remaining $\sim 50\%$ of the UVB were contributed by faint, undetected galaxies; however this appears to violate limits from the fluctuations in the UVB measured in the HDF (Vogele 1997). Despite these uncertainties, the approximate amplitude of the UVB allows us to compute useful estimates of the contribution of IG dust to the FIRB.

The rest of this paper is organized as follows. In § 2 we summarize our model for the amount and type of IG dust; in § 3 we describe our assumptions concerning the redshift evolution of both the UV emission and dust production, and outline our calculation methods; and in § 4 we discuss limits from existing FIRAS observations of the CMB. Section § 5 contains our main results on the contribution to the FIRB from IG dust, as well as hopes for future tests of the dust hypothesis for the SN results; and, in § 6 we summarize our conclusions. Unless otherwise stated, in this paper we adopt an open cosmology with total matter density $\Omega = 0.2$ and Hubble constant $h_{50} = 1$.

2. IG DUST MODEL

The model adopted here for IG dust is discussed at length in A99; here we provide only a brief summary. The model is based on the following method of estimating the total IG dust density $\Omega_{\text{dust}}(z)$: we first estimate the total metal density $\Omega_Z(z)$, then multiply this figure by the fraction F_I of these metals which lie outside galaxies, and then by the fraction d_m of IG metals is contained in IG dust.

As shown in A99, both a direct integration of the SFR (with an assumption of the metals produced for each star formed) and fossil evidence from clusters indicate that $\Omega_Z(z \lesssim 0.5) \approx (2.5 - 5) \times 10^{-4}$ (adjusted from A99 for $h_{50} = 1$). These estimates follow from conservative as-

sumptions: that stars in cluster galaxies have the same IMF as in field galaxies, that there is not a dominant population of unobserved galaxies, etc.; see A99.

Measurements of the metallicity of intracluster gas indicate that a fraction $F_I \approx 75\%$ of a typical cluster’s metals lie in the intracluster medium (e.g. Renzini 1997), presumably removed from the galaxies by some combination of winds, dust expulsion, ram-pressure stripping, and tidal disruption/merging of galaxies. While ram-pressure stripping and mergers may be more effective at removing metals from cluster galaxies, it is nevertheless likely that the figure $F_I \approx 75\%$ applies to the field galaxies, since a much smaller value, together with the estimate of $\Omega_Z \gtrsim 10^{-4}$, would imply that field galaxies have mean metallicity several times solar – contrary to observation.

To estimate the fraction d_m of IG metals in dust, we assume a value of d_m 0.5 for metals leaving the galaxy, as applies to the interstellar medium of both typical galaxies and perhaps even to damped Ly- α systems (Pei, Fall & Hauser 1998). Some fraction $(1 - f)$ by mass of this dust must be destroyed either during ejection or in the IG medium, giving $d_m \approx 0.5f$. Combining these figures, we estimate an IG dust density at $z \lesssim 0.5$ of

$$\Omega_{\text{dust}} \approx (9.4 - 18.8)f \times 10^{-5}. \quad (1)$$

To fix both f and the dust properties, we shall adopt the two-component Draine & Lee (1984) [DL] dust model¹ of silicate and graphite spheres with size distribution $N(a)da \propto a^{-3.5}$, $0.005 \mu\text{m} \leq a \leq 0.25 \mu\text{m}$ (Mathis, Rumpl & Nordsieck 1977 [MRN]) as representative of galactic dust. We further assume that IG dust differs from MRN dust due to the removal – by the selective ejection of large grains and/or the selective destruction of small grains by sputtering – of the small-size end of the grain-size distribution. In this paper we use absorption and scattering curves as calculated in Laor & Draine (1993), and the truncated MRN distribution with $a_{\text{min}} = 0.1 \mu\text{m}$; The minimal grain size (which corresponds to $f \approx 0.4$) is chosen to give dust which is grey enough not to over-redden the supernovae (A99). Note that our results should not be sensitive to our adoption of the Milky Way dust cross section - e.g. LMC dust differs from Milky Way dust mainly at short wavelengths, where the opacity has anyway been modified by removing the small grains. Silicate and graphite grains are assumed to have equal mass densities, and the total dust density is chosen, according to the cosmology, as that sufficient to reconcile the chosen cosmology with the supernova results. For example, $\Omega = 0.2$ requires $\sim 0.15 - 0.2$ mag of extinction at $z \sim 0.5$ and hence $\Omega_{\text{dust}} \sim (5.5 - 7) \times 10^{-5}$ to be consistent with the observations.

3. METHOD OF CALCULATION

In estimating the contribution from IG dust to the FIRB and the CMB, we follow the methods of Wright (1981) (see also Loeb & Haiman 1997). We define the comoving number density of photons at redshift z and comoving frequency ν as

$$N_\nu(z) \equiv \frac{4\pi}{hc(1+z)^3} J_{\nu(1+z)}(z), \quad (2)$$

¹The effects are, of course, somewhat dependent upon the grain model; see A99 for discussion.

where $J_\nu(z)$ is the usual specific intensity of the background radiation field in physical (non-comoving) units of $\text{erg cm}^{-2} \text{s}^{-1} \text{Hz}^{-1} \text{sr}^{-1}$. The evolution of $N_\nu(z)$ with redshift is then described by the cosmological radiative transfer equation

$$-\frac{dN_\nu(z)}{dz} = \frac{c}{dz} \frac{dt}{dz} [j_{\text{tot},\nu}(z) - \alpha_\nu(z)N_\nu(z)] \quad (3)$$

where $j_{\text{tot},\nu} = j_{\star,\nu} + j_{\text{dust},\nu}$ is the total comoving emission coefficient, including both the direct light of UV sources $j_{\star,\nu}$ (see equation 8 below), as well as thermal dust emission $j_{\text{dust},\nu}$ from dust. As discussed in section § 2 above, we assume that dust is composed of graphite and silicate grains, so that the total dust absorption coefficient, $\alpha_\nu = \alpha_{\text{Si},\nu} + \alpha_{\text{Gr},\nu}$ is given in units of cm^{-1} by

$$\alpha_\nu(z) = \rho_{\text{Si}}(z)\kappa_{\text{Si},\nu(1+z)} + \rho_{\text{Gr}}(z)\kappa_{\text{Gr},\nu(1+z)} \quad (4)$$

for a total mass density of $\rho_{\text{Si}} + \rho_{\text{Gr}} = (\Omega_{\text{Si}} + \Omega_{\text{Gr}})\rho_{\text{crit},0}(1+z)^3$ in dust, where the κ 's are the dust opacities in units of $\text{cm}^2 \text{g}^{-1}$. Note that by assumption, $\Omega_{\text{Si}} = \Omega_{\text{Gr}}$. The total comoving dust emission coefficient is then

$$j_{\text{dust},\nu} = j_{\text{Si},\nu} + j_{\text{Gr},\nu} \quad (5)$$

$$= \frac{8\pi\nu^3}{c^3} \left\{ \frac{\alpha_{\text{Si},\nu}(z)}{\exp[h\nu(1+z)/k_{\text{B}}T_{\text{Si}}] - 1} + \frac{\alpha_{\text{Gr},\nu}(z)}{\exp[h\nu(1+z)/k_{\text{B}}T_{\text{Gr}}] - 1} \right\}. \quad (6)$$

The silicate and graphite grains are assumed to be separately in thermal equilibrium with the total background radiation (CMB + UV sources), so that the grain temperatures T_i are obtained by equating the total amount of absorption and emission:

$$\int_0^\infty d\nu \alpha_{i,\nu} N_\nu(z) = \int_0^\infty d\nu j_{i,\nu}, \quad (7)$$

where $i = \text{Si}$ or Gr .

The infrared background spectrum arises from the re-emission of UV light absorbed by dust. The two main factors determining the FIRB are therefore the evolution of the UV emissivity $j_{\star,\nu}$ from stellar sources (determining the dust temperature), as well as the evolution of the dust density, $\Omega_{\text{dust}} = \Omega_{\text{Si}} + \Omega_{\text{Gr}}$ – determining the overall amplitude of the emissivity. For the UV production rate, here we adopt the global average star-formation rate as determined recently by Madau et al. (1998). We ignore any additional UV flux from quasars: at the redshifts of interest here ($z \lesssim 5$), the contribution to the UV background from the known population of quasars is less than 20% (M99). Note, however, that a population of faint, undetected quasars could contribute substantially to the UV background (Haiman & Loeb 1998).

For simplicity, we assume further that the average spectrum from the stellar UV sources is described as that of black-body radiation at a temperature of $T = 9000\text{K}$. This is a reasonably good approximation to the continuum in the composite spectra found in the population synthesis models of Bruzual & Charlot (1996), although the pure black-body spectrum is somewhat narrower. The black-body also falls below the UV background flux limit at the

shortest wavelengths ($\lambda \sim 0.1 \mu\text{m}$); see also § 3. Our results below depend primarily on the total amount of stellar light absorbed by the dust, and are insensitive to the precise shape of the UV spectrum (see detailed discussion below). With the above assumptions, the stellar emissivity is given by

$$j_{\star,\nu}(z) = A_{\text{uv}} \dot{\rho}_\star(z) B_\nu(T = 9000\text{K}), \quad (8)$$

where B_ν is the Planck function, and $\dot{\rho}_\star(z)$ is the star formation rate in Madau et al. (1998), converted from their standard $\Omega = 1$ cosmology to the open $\Omega = 0.2$ model assumed here, using the multiplicative factor $(dv_o/d_{l,o}^2)/(dv_\Lambda/d_{l,\Lambda}^2)$, where d_v and d_l are the volume elements and luminosity distances in the two cosmologies (Eisenstein 1997).

The overall normalization constant A_{uv} is somewhat uncertain. M99 argues that the total UV produced by stars is a factor ~ 2 smaller than the recent measurement of the extragalactic UV background, $J_\nu = 20 \text{ nW m}^{-2} \text{sr}^{-1}$ at $0.55 \mu\text{m}$ by Bernstein (1997). It is not clear what the reason for this discrepancy is; the shortage of UV could be provided by additional faint galaxies or quasars (however, see Vogeley 1997). Here we take the simplest approach, and adjust the normalization constant A_{uv} so that the measured value of $20 \text{ nW m}^{-2} \text{sr}^{-1}$ for the UV background at $0.55 \mu\text{m}$ is exactly reproduced (taking into account dust absorption). Given the shortage of UV provided by the known stellar population, we will also examine below a model normalized to $10 \text{ nW m}^{-2} \text{sr}^{-1}$, the lower end of the 1σ range quoted by Bernstein (1997). This also lies above the lower limits on the UV background derived from galaxy counts in the Hubble Deep Field (Pozzetti et al. 1998; see figure 2). Note that we have assumed a specific spectral shape and redshift-evolution of the UV emissivity. We again emphasize that our results are insensitive to the detailed shape of the UV flux around $1 \mu\text{m}$, and depend only on the total amount of UV light absorbed; this is demonstrated by a model we examine below with a more realistic spectrum obtained from population synthesis models (Bruzual & Charlot 1996) and models with SF histories different from M99. As mentioned above, the difference between the background inferred from the observed star-formation rate (i.e. by direct integration of $\dot{\rho}_\star$ and an empirical UV flux per stellar mass ratio), and the measured value of $20 \text{ nW m}^{-2} \text{sr}^{-1}$ could be provided by undetected quasars, or other yet undiscovered sources. As long as the redshift evolution of these sources does not depart significantly from the range of our assumed $\dot{\rho}_\star(z)$'s, our results below would remain valid.

Next, we assume that the same stellar population that produces the UV background is the source of IG dust. Under this simple assumption, the mass density of dust increases in proportion to the mass density in stars:

$$\Omega_{\text{dust}}(z) = A_{\text{dust}} \int_{t(z=10)}^{t(z)} dt \dot{\rho}_\star(z), \quad (9)$$

and we assume further that $\Omega_{\text{Si}} = \Omega_{\text{Gr}} = \Omega_{\text{dust}}/2$, as is the case in the Milky Way (see discussion in § 2 above). The normalization constant A_{dust} is chosen by requiring the total optical depth due to dust absorption + scattering between $z = 0$ and $z = 0.5$ to be ~ 0.15 . As we

argued in section § 1 above, this is the amount needed to account for the SN results (A99). This normalization corresponds to $\Omega(z=0) \sim 5 \times 10^{-5}$. Adding to the arguments given in § 1, we note that this dust density fits in comfortably with the amount of dust expected to be produced in normal stars. For instance, assuming that each type II SN ($M_* \geq 8M_\odot$) yields $0.3M_\odot$ of dust, adopting a Scalo IMF, and normalizing $\Omega_*(z=0) = 0.004$; we obtain $\Omega(z=0) = 5 \times 10^{-5}$ (cf. Loeb & Haiman 1997). This estimate does not account for dust trapped in galaxies or destroyed, but is also a lower limit since it only includes the dust formed in supernovae, and not that formed in (for example) dense clouds or carbon stars.

We note that although stellar dust production cannot occur instantaneously with star-formation, the relevant time-scales are likely to be much shorter than the Hubble time at redshifts of interest. Type II SNe produce dust in a few million years; while the lifetime of carbon stars (believed to be dominating the dust budget in the Milky Way, see Gehrz 1989) is still only ~ 1 Gyr. The ejection timescale for dust leaving spiral galaxies is probably between 100 and 1000 Myr (A99). We have found that incorporating a delay of ~ 1 Gyr between star formation and dust production into equation 9 does not change our results below by more than a few percent.

Equations 2-9, together with the initial condition that N_ν at some high redshift is equal to the pure CMB with $T_{\text{cmb}} = 2.728(1+z)\text{K}$, determine the redshift evolution of the full background spectrum.

4. EXISTING FIRAS LIMITS

Any existing IG dust component will process some UV/optical energy into the FIR/microwave. As a result, some (perhaps vanishingly small) fraction of the observed CMB is due to emission from IG dust. This contribution has been studied a number of times previously. Some authors have investigated the possibility that the CMB is entirely dust-processed emission from astrophysical objects; see, e.g., Layzer & Hively (1973), Wright (1982), Wollman (1992) and Aguirre (in preparation) on ‘cold big-bang’ models, or Wickramasinghe et al. (1975), and Hoyle & Wickramasinghe (1988) on steady-state models. In cold big-bang models, thermalization takes place at very high z after energy emission by Population III objects. Both cosmologies require grains of a type that can maintain a temperature very close to that of the CMB.

If the grains have a temperature only slightly different from that of the CMB, they will be too cool to contribute to the FIRB; however, spectral distortions of an initially blackbody CMB will occur (e.g. Rowan-Robinson, Negroponte & Silk 1979; Hawkins & Wright 1988; Bond et al. 1991). More recently, this effect has been used by Loeb & Haiman (1997) and by Ferrara et al. (1999) to limit the density of IG dust. We shall perform a similar analysis using the method and assumptions outlined in § 3, and with the dust model described in § 1.

Models which distort the CMB at long ($\gg 1\text{mm}$) wavelengths can be easily constrained since there is a clear model for the CMB (perfect blackbody). But in the ab-

sence of an equally unique and well-defined model for the FIRB, it is much less clear how to limit FIR emission that does not actually exceed the observed FIR background. The procedure adopted here is as follows: following the methodology of Fixsen et al. (1996), we fit the results from $500 - 5000 \mu\text{m}$ by a blackbody $B_\nu(T_{\text{cmb}})$ plus a ‘uniform dust component’ parameterized by an emissivity and temperature in a $\nu^2 B_\nu(T)$ spectrum. These fitted components are shown in dotted lines in Figure 2. The spectrum with the CMB *only* subtracted is shown as a solid line; this makes clear the contribution of IG dust emission to the FIRB. The residuals with both components subtracted are shown in the second panel, along with the FIRAS frequency range (vertical dotted lines) and the limit on r.m.s. deviations from blackbody (horizontal dotted line).

An interesting note about this general procedure is the following. Our calculations show that the fitted CMB temperature may be close to, but not exactly the same as the actual initial CMB, and this small discrepancy affects the measured slope of the FIR emission at $\lambda \gtrsim 850 \mu\text{m}$, since the FIRB is $\lesssim 1/1000$ of the CMB flux there. For example, fitting the CMB plus $\nu^2 B_\nu$ gives a fitted CMB temperature of 2.72800K , exactly as it should be. But if we fit a CMB plus $\nu^{0.64} B_\nu$ (the shape of the FIRAS fit), we find $T_{\text{cmb}} = 2.72795\text{K}$. The CMB is then slightly under-subtracted, and the residual FIRB closely follows a $I_\nu \propto \nu^{3.64}$ shape at long- λ . This suggests that accurately determining the slope of the FIRB long-wavelength tail requires knowledge of T_{cmb} to much higher accuracy than available from COBE data. For this reason, we find it is not useful to compare the FIRB slope predicted by models to the FIRAS fit, for $\lambda \gtrsim 850 \mu\text{m}$.

Table 1 gives the r.m.s. deviation from blackbody for the computed spectra, with the mean taken over the $500 \mu\text{m} \leq \lambda \lesssim 5000 \mu\text{m}$ wavelength range analyzed by Fixsen et al. (1996) and divided by the peak of $B_\nu(T_{\text{cmb}})$. The limit given by Fixsen et al. 1996 on this number is 5×10^{-5} . The result of this analysis is that the dust emission would not cause detectable distortions to the CMB for the dust model described, despite the fact that they appear to violate the quoted limits on the y parameter and r.m.s. distortion.² The residuals are, of course, even smaller if the ‘uniform dust component’ is fit using a free index in the power law.

On the other hand, modification of the long-wavelength opacity of the dust can be important, since dust types with higher FIR opacity have lower equilibrium temperatures which may lead to excessive emission into the FIRB/CMB. Since the dust emission tends to be well described by the fitted $\nu^2 B_\nu$ isotropic dust component, this emission does not tend to leave excessive distortion in the CMB residuals. Rather, it leads to a fit of the isotropic dust component incompatible with that found by FIRAS. Accordingly, we discuss these models in the next section, which treats the dust contribution to the FIRB and the resulting limits on the dust models.

5. IG DUST CONTRIBUTION TO THE FIRB

²In light of the uncertainty in the FIRB, it seems that the quoted limits on r.m.s. distortions and the y -parameter from the COBE group are somewhat misleading. Rather large spectral distortions can be ‘hidden’ in the microwave tail of the FIRB which has a poorly defined spectral shape. Assuming conservatively that the FIRB as detected by FIRAS exists in the 150-600 GHz range (and zero outside), it corresponds to a y -parameter in the full 60-600 GHz interval of 2×10^{-4} , over an order of magnitude above the quoted upper limit.

In this section, we analyze the contribution by IG dust emission to the FIRB in a variety of models. Section § 5.1 presents and discusses our fiducial model. Section § 3 lists possible variations in the parameters, and discusses the effects of these variations, and section § 4 discusses how resolution of the FIRB into discrete sources by future experiments would improve the constraints.

5.1. Fiducial Model

In our fiducial model, the cosmology is open, with $\Omega = 0.2$ and $h_{50} = 1$. The star formation rate is taken from M99 and shown in A99, Figure 1. The dust has equal parts by mass in silicate and graphite grains with $a_{\min} = 0.1 \mu\text{m}$, and density proportional to the integrated SFR, normalized to $\Omega_{\text{dust}}(z=0) = 5.4 \times 10^{-5}$, which gives 0.15 mag of extinction to $z = 0.5$ at (observed) $0.66 \mu\text{m}$. The galaxy spectrum is a 9000 K blackbody, normalized to give $20 \text{ nW m}^{-2} \text{ sr}^{-1}$ after dust processing at $0.55 \mu\text{m}$.

The predictions of the fiducial model appear in Figure 2 and Table 1. The figure shows the complete final spectrum with the CMB (fit using the method of § 2) subtracted. For comparison we also include the UVB lower limits (Pozzetti et al. 1998) and detections (Bernstein 1997), the DIRBE FIRB upper limits and detections (Hauser et al. 1998), and the FIRAS detections (Fixsen et al. 1998) with $\pm 1\sigma$ uncertainties. It is apparent that the dust emission contributes significantly to the long-wavelength flux – in fact it can account for all of the $850 \mu\text{m}$ flux given by the FIRAS measurements – but fails to reproduce the shape or amplitude of the entire FIRB. This is specified quantitatively in Table 1, where the fifth and sixth columns list the numerical fraction of the FIRAS FIRB measurements that the dust emission would contribute at 200 and $850 \mu\text{m}$. These numbers should be multiplied by 0.54 to yield the fraction of the 1σ upper limit on the FIRB, or 1.25 to account for the minimum 20% resolved fraction. Column seven lists the y -parameter represented by the FIR emission, defined by $y \equiv 0.25(u_{\text{tot}}/u_{\text{cmb}} - 1)$, where u_{tot} and u_{cmb} are the total energy density and the energy density of the CMB alone, both evaluated in the 60-600 GHz frequency range. This gives a measure of the total dust energy output. The last column gives the r.m.s. residual after both CMB and the $\nu^2 B_\nu$ fit to the FIR emission are subtracted, as discussed in § 2.

The next section analyzes the possible variations upon these predictions resulting from changes in the model. Some of the variations can be ruled out because they predict a FIRB contribution above the FIRAS limit; these models could be saved only if the FIRAS team has over-subtracted the foreground contribution. Stronger limits can be obtained on the various models by considering their contribution to the *unresolved* fraction of the FIRB, after the contributions by known discrete sources are subtracted. These constraints will be discussed in section 4 below.

5.2. Variations on the model

Several variations were performed to test the robustness of our model assumptions. First, raising H_0 from 50 to

$80 \text{ km s}^{-1} \text{ mpc}^{-1}$ (model H80) made very little difference. Second, an SFR which is flat for $z > 3$, but unchanged for $z < 3$ was employed (model FSFR). This choice is motivated by the “effective” global average SFR (M99) required to reionize the universe by $z = 5$. This increases the dust contribution to the final spectrum by about 35%, and the $850 \mu\text{m}$ contribution by 45%. The change occurs because relatively more of the UV energy is emitted at high z , where the dust is more dense, and emits into longer (rest-frame) wavelengths.

Next, we tested the adequacy of our assumption of the single-temperature blackbody galaxy spectrum, by using a more realistic spectral template. We utilize the Bruzual-Charlot (1996) starburst population synthesis model with a Scalo IMF to compute the shape of spectrum as a function of the age of the population. This time-dependent template is convolved with the SFR from M99 to find the redshift-evolution of the frequency dependent UV emissivity. The full spectrum under these assumptions is shown by the curve labeled “BC” in Figure 3. The peak in the UVB from the direct galactic emission is broader than in our fiducial model, and extends to higher energies. As mentioned above, this procedure results in a UVB at $z = 0$ that falls short of the measured value by a factor of ~ 2 . Overall, the contribution to the FIRB is not effected significantly: it is reduced only by $\sim 10\%$ relative to our fiducial model at $850 \mu\text{m}$ (cf. Table 1).

It must be noted that the above procedure is not strictly correct, as we have not corrected the galactic templates for reddening by dust internal to the galaxy. This reddening could be important in the present context, since it makes the UV peak steeper in the $0.1 - 1 \mu\text{m}$ range, and allow a broader UVB in this wavelength range that reaches $\sim 20 \text{ nW m}^{-2} \text{ sr}^{-1}$ at $0.55 \mu\text{m}$, while extending to energies higher than assumed in our fiducial model. Here we do not attempt to derive an accurate reddening correction (see instead Madau et al. 1998). Rather, our aim is to assess the maximum UV flux that could, in principle, be present in the $0.1 - 1 \mu\text{m}$ range, that is consistent with both the Voyager upper limit (Murthy, Henry & Holberg 1998) and the $0.55 \mu\text{m}$ detection.

To compute this maximal UV flux, we reddened the galactic template spectrum, assuming the cross section of Milky Way dust (DL), with a total (unrealistically high) maximum optical depth of ~ 4 . We then re-scaled the UV efficiency by a factor of ~ 10 to retain a flux of $\sim 20 \text{ nW m}^{-2} \text{ sr}^{-1}$ at $0.55 \mu\text{m}$. The resulting spectrum is shown by the curve labeled “BC2” in Figure 3. This spectrum fits in with both the Voyager and Bernstein (1997) data points, and reasonably represents the maximally allowed UV emission. It is interesting to note that a simultaneous fit to these two data-points requires a very steep spectrum ($20 \text{ nW m}^{-2} \text{ sr}^{-1}$ at $0.55 \mu\text{m}$ to $0.6 \text{ nW m}^{-2} \text{ sr}^{-1}$ at $0.1 \mu\text{m}$, implying a slope of $I \sim \lambda^2$), which can only be derived from the Bruzual-Charlot template by postulating an exceedingly high reddening. One resolution of this paradox might be that the true value of the UVB is closer to $10 \text{ nW m}^{-2} \text{ sr}^{-1}$ (as argued by Vogeley 1997 in a different context). We find that with this maximal emission, the FIRB contribution increases somewhat, but the change is once again not significant, only $\sim 40\%$ relative to the galactic model without reddening, over-predicting the $850 \mu\text{m}$ FIRB by $\sim 26\%$ (cf. Table 1), but still well

TABLE 1
INTERGALACTIC DUST EMISSION MODELS

Model	Variation	T_{Gr}	T_{Si}	f_{200}	f_{850}	$y_{\text{FIRB}}/10^{-4}$	rms/ 10^{-6}
Fid.	-	9.9	7.3	0.14	1.02	2.0	3.7
H80	$H_0 = 80 \text{ km s}^{-1} \text{ mpc}^{-1}$	9.9	7.3	0.15	1.10	2.1	4.0
FSFR	SFR flat for $z > 3$	9.9	7.3	0.16	1.45	2.7	7.4
BC	Galaxy spectra from Bruzual-Charlot	9.3	7.8	0.08	0.89	1.7	2.9
BC2	Bruzual-Charlot + extreme reddening	10.5	7.9	0.24	1.26	2.5	4.6
MG	$a = 0.1 \mu\text{m}$ grains, $\Omega_d = 4.5 \times 10^{-5}$	10.2	7.1	0.17	0.96	1.9	3.4
LG	$a = 0.25 \mu\text{m}$ grains, $\Omega_d = 7.6 \times 10^{-5}$	9.2	7.4	0.08	0.85	1.6	3.1
LUV	UVB of $10 \text{ nW m}^{-2} \text{ sr}^{-1}$ at $0.55 \mu\text{m}$	8.8	6.5	0.05	0.72	1.3	2.5
SCDM	$\Omega = 1$, $\Omega_d(z=0) = 1.25 \times 10^{-4}$	9.9	7.3	0.30	1.94	3.8	6.7
SCDMb	SCDM, but UVB of $10 \text{ nW m}^{-2} \text{ sr}^{-1}$	8.8	6.5	0.10	1.33	2.5	4.4
G05	κ flat to $\lambda_0 = 0.5 \mu\text{m}$	17.3	-	0.86	0.45	1.1	1.1
G2	κ flat to $\lambda_0 = 2 \mu\text{m}$	12.8	-	0.88	1.56	3.5	4.6
G5	κ flat to $\lambda_0 = 5 \mu\text{m}$	9.7	-	0.53	3.97	7.8	12
G10	κ flat to $\lambda_0 = 10 \mu\text{m}$	7.7	-	0.24	7.71	13.4	19
L1.0	$\kappa(\lambda \geq 100 \mu\text{m}) \propto \lambda^{-1}$	7.9	5.5	0.038	2.59	4.4	18
L1.5	$\kappa(\lambda \geq 100 \mu\text{m}) \propto \lambda^{-1.5}$	9.0	6.4	0.083	1.71	3.1	9.5
L2.5	$\kappa(\lambda \geq 100 \mu\text{m}) \propto \lambda^{-2.5}$	10.6	8.0	0.19	0.65	1.3	1.7
GRA	graphite, $a_{\text{min}} = 0.05 \mu\text{m}$	9.8	-	0.21	1.29	2.6	4.4

within the $+1\sigma$ uncertainty.

Third, we have tested our assumption that we may treat the grain-size distribution as a single component, by considering grains of a single grain size a , for $a = 0.1 \mu\text{m}$ (model MG) and $a = 0.25 \mu\text{m}$ (model LG). These extremes change the $z = 0$ temperature by $0.1\text{--}0.7 \text{ K}$ and the $850 \mu\text{m}$ flux by $\lesssim 4\text{--}15\%$, demonstrating that the approximation is not very important. The test also shows that the results are not sensitive to the grain size distribution, as long as all of the grains are relatively large ($a \gtrsim 0.1 \mu\text{m}$).

Finally, we check our assumption that the dust temperature follows from equilibrium with a homogeneous background radiation bath, because dust near concentrations of radiation could have somewhat higher temperature. To determine whether this might be important, we have computed the critical distance $r_{\text{crit}}(z)$ (from center of a model galaxy) at which a dust grain would feel equal contributions from the cosmic UVB intensity $J_\nu(z)$ and from the nearby galaxy, i.e.

$$4\pi(1+z)^3 J_\nu = \frac{L_{\text{gal}}}{4\pi r_{\text{crit}}^2}, \quad (10)$$

where the galaxy luminosity $L_{\text{gal}} \sim 10^{46} \text{ erg s}^{-1}$ (corresponding to a $10^{12} M_\odot$ starburst galaxy, with the spectral model of Bruzual & Charlot 1996) is constant and $J_\nu(z)$ is proportional to the integrated comoving SFR and has the value $20 \text{ nW m}^{-2} \text{ sr}^{-1}$ at $z = 0$. The result is that $r_{\text{crit}} \lesssim 60 \text{ kpc}$ for all z and $r_{\text{crit}} \lesssim 30 \text{ kpc}$ for $z > 1$. In A99, it was argued that IG dust must be $\gtrsim 70 \text{ kpc}$ from its progenitor galaxy to be uniform enough to be in accord with limits on the dispersion in supernova brightnesses. Thus even near extremely bright galaxies, dust of the A99 model should have temperature dominated by the isotropic background rather than nearby galaxies.

As discussed in §3, there are still sizeable uncertainties in the normalization of the UV spectrum. The 1σ lower limits from Bernstein (1997) roughly coincide with the lower limits given by integrated counts (M99) at $\sim 10 \text{ nW m}^{-2} \text{ sr}^{-1}$ at $0.55 \mu\text{m}$. We have employed this normalization (model LUV), and find that this lowers the $850 \mu\text{m}$ flux by about 30% (the decrease in energy is somewhat offset by the lower temperature of the dust).

Although most models considered predict an $850 \mu\text{m}$ flux comparable to that detected by FIRAS, some models exceed the FIRAS upper limit. To reconcile the supernova measurements with a closed, matter-dominated cosmology – such as the standard cold dark matter model (SCDM) – an extinction of $A_V(z \sim 0.5) \sim 0.35 \text{ mag}$ is required (A99), in turn requiring $\Omega_d(z=0) \approx 1.25 \times 10^{-4}$ for $h_{50} = 1$. In the present model this predicts an $850 \mu\text{m}$ flux which exceeds the $1 - \sigma$ bound of the FIRAS detection (see the SCDM model in Table 1.) With the lower UV normalization, however, the emission falls within the errors (model SCDMb in Table 1). If the higher UV normalization holds, these results make it rather unlikely that IG dust could reconcile SCDM with the supernova observations, even if the large necessary quantity of dust existed (cf. A99).

The present calculations can also constrain the properties of intergalactic dust if it is assumed to be responsible for the supernova dimming. Very grey dust, for instance, absorbs more UV/optical flux for a given V-band extinction (and can hence overproduce the FIRB). Both very grey dust and ‘standard’ dust with high IR emissivity can also have lower equilibrium temperature, which overproduces the FIRB at long wavelengths. To limit these sorts of dust, we have considered two illustrative types. The first is dust that is grey out to some wavelength λ_0 , then

falls as λ^{-2} :

$$\kappa_\lambda \propto \frac{1}{[1 + (\lambda/\lambda_0)^2]}. \quad (11)$$

This is conservative in the sense of ensuring the maximum reasonable temperature for a given λ_0 . Models (G05-G10) are of this type, and show that for $\lambda_0 \gtrsim 3 \mu\text{m}$ the FIRB is overproduced. It is interesting to note, however, that $\lambda_0 \approx 0.5$ models actually produce a FIRB fitting the observations rather well over the entire frequency range. Conducting needles have an absorption spectrum which can be roughly modeled by eq. 11 (Wright 1982; Wickramasinghe & Wallis 1996; Aguirre 1999a), and using Wright's 1982 RC model with a resistivity of $\sim 10^{-15}$ s, we can rule out needle models with length-to-diameter ratio $L/d \gtrsim 6$.³

The second dust type is 'standard' DL/MRN dust, but with long-wavelength ($\lambda \gtrsim 100 \mu\text{m}$) emissivity given by $\kappa_\lambda \propto \lambda^{-\alpha}$ with $\alpha \neq 2$. Fluffy/fractal grains can give $\alpha \sim 1$ (e.g. Wright 1987; Stognienko et al. 1995), and α generally depends upon the optical properties of the grain material. Dust with $\alpha < 2$ generally has lower temperature, and the calculations (see models L1.0, L1.5 in Table 1) show that such dust will overproduce the $850 \mu\text{m}$ FIRB (at the 1σ level) for $\alpha \lesssim 1.5$. On the other hand, if dust had $\alpha > 2$, model L2.5 shows that the higher resulting temperature would lead to less flux at $850 \mu\text{m}$. The comoving dust temperature $T_{\text{dust}}/(1+z)$ for the fiducial model and models GR05 and L1.0 is shown in Figure 1. All computed models fall within the range spanned by the GR05 and L1.0 models.

In summary, using only the FIRAS limits on the FIRB, we can with some confidence rule out SCDM models, 'very grey' dust models with $\lambda_0 \gtrsim 3 \mu\text{m}$, and dust models with lower law index $\lesssim 1.5$ in their long-wavelength emissivity. The next section discusses stronger constraints which derive from the fraction of the measured FIRB which is known to be due to discrete sources.

5.3. Resolving the FIRB: Tests and future observations

When constraining models using their predicted IG dust contribution to the FIRB, we have so far considered the full value of the FIRB. However, as mentioned above, we already know that the entire FIRB cannot be comprised of IG dust emission alone. On the one hand, the IG dust models generally fail to produce the short wavelength fluxes; on the other hand, observations have already resolved a non-negligible fraction ($\gtrsim 25\%$) of the FIRB into discrete sources. If 20 – 30% of the FIRB is accounted for by resolved sources, the numbers in column six of Table 1 should be multiplied by 1.25-1.5, as only 70 – 80% of the measured FIRB can be IG dust emission. To use instead the 1σ upper limit on the detected FIRB, but taking into account the resolved fraction, column six should be multiplied by 0.6 – 0.64. Resolving the FIRB further could provide significantly stronger constraints on the models.

At the present time, a handful (~ 30) of objects with fluxes S above $S \geq 2 \text{ mJy}$ at $850 \mu\text{m}$ have been detected by SCUBA. These data have been used to derive the empirical number counts $n(S)$ of sources, as a function of apparent

flux. At the limiting flux of $S = 2 \text{ mJy}$, the total contribution from these objects is a fraction 20 – 30% of the FIRB value (Barger et al. 1999a). As emphasized by these authors, the faint-end counts are very steep ($n(S) \propto S^{-3.2}$). Extrapolating at the faint end of the number counts to $\sim 0.5 \text{ mJy}$ would then account for the entire measured background. These conclusions are further supported by the somewhat less reliable detections of faint sources down to $\sim 1 \text{ mJy}$: the gravitationally lensed sample of Blain et al. (1999) extends to this limit, albeit with only a single source fainter than $\sim 2 \text{ mJy}$.

In light of these existing measurements, and especially because of the steepness of the faint-end number counts, tightening the constraints obtained in this paper requires relatively small further improvements in the observations. In particular, with a faint-end slope of -3.2, the flux limit needs to be lowered only by a factor of four, to $\sim 0.5 \text{ mJy}$, to detect the sources that account for the whole of the FIRB, provided these sources exist. If the faint sources do not exist, then these measurements will find the turn-over and flattening in $n(S)$, and yield the actual fraction of the FIRB not accounted for by these sources. If the faint sources are detected, the uncertainty in their total cumulative flux would be relatively small, since these sources are expected to be numerous.

A complication we have ignored in this analysis is the following: most IG dust emission occurs at $1 \lesssim z \lesssim 3$, where a tentative redshift analysis (Barger et al. 1999b) indicates that most of the SCUBA $850 \mu\text{m}$ sources lie. The source fluxes are derived using a 30 arcsec aperture, which at $z > 1$ corresponds to a physical size of $\gtrsim 250 h_{65}^{-1} \text{ kpc}$. We have assumed for simplicity that the IG dust is effectively uniform, but at $z > 1$ significant quantities could be within 125 kpc of galaxies, so there is a danger that the SCUBA derived fluxes include some emission from what we have termed IG dust. Upcoming sub-mm surveys with better angular resolution should be able to clarify this ambiguity.

In summary, with a factor of four improvement over the current SCUBA detection threshold, we would either see explicitly the need for something else to explain the FIRB, or else a fairly tight constraint on the IG dust will be possible. Forthcoming instruments such *Bolocam* and *SIRTF* will reach the required sensitivities at $160 \mu\text{m}$ and $1100 \mu\text{m}$ (see Table 1 in Blain 1999). The constraints that can be obtained then might then be limited by the accuracy of the absolute measurement of the coarse-grained FIRB. The High Frequency Instrument (HFI) on the future Planck satellite⁴, covering the $350 - 3000 \mu\text{m}$ range at several intermediate frequencies, will be able to greatly improve our existing knowledge of the unresolved component. Finally, as shown by Haiman & Knox (1999), angular correlations in the FIRB are expected to be at the few percent level, and depend strongly on the nature of its sources. Future instruments such as *BLAZE* and *FIRBAT* will be able to measure these correlations, providing another diagnostic that distinguishes between IG dust and discrete sources.

6. CONCLUSIONS

³Needles with high L/d and high conductivity, such as the iron whiskers of Hoyle & Wickramasinghe (1988), can maintain a temperature very close to that of the CMB and are not constrained by the present calculations; see also Aguirre (in preparation).

⁴See <http://astro.estec.esa.nl/SA-general/Projects/Planck>.

In this paper, we studied the far infrared emission from the type and amount of IG dust necessary to explain the recent Hubble diagrams, derived from observations of Type Ia SNe at redshifts $0 < z < 1$, in cosmological models without a cosmological constant. In particular, we computed the contribution from the IG dust emission to the value of the FIRB recently measured by the COBE satellite. We investigated a broad range of models, and focused on the wavelength of $850\ \mu\text{m}$, where the largest fraction of the FIRB is presently resolved into discrete sources, thus yielding the strongest constraints.

Our results show that the IG dust emission is consistent with the spectral distortion of the CMB allowed by present COBE data, but would contribute a substantial fraction ($\gtrsim 70\%$) of the *unresolved* fraction of the FIRB in the $300 - 1000\ \mu\text{m}$ range. In a few specific models, this contribution is sufficiently large to render those models im-

plausible, including Standard CDM and models with very grey dust, or dust with unusually high IR emissivity. In the (perhaps most interesting) case of an open universe with a low matter density ($\Omega = 0.2$), we find that the contribution is still within the experimental uncertainty. Assuming that 20% of the FIRB is accounted for by the discrete SCUBA sources, the IG dust contributes $\sim 70\%$ of the $+1\sigma$ limit on the *unresolved* fraction. Future observations of the far infrared background by Planck, and its discrete constituents by *SIRTF* and *Bolocam* will provide a definitive test of the IG dust hypothesis.

We thank P. Madau for providing a fitting formula for the SFR. ZH was supported by the DOE and the NASA grant NAG 5-7092 at Fermilab. This work was supported in part by the National Science Foundation grant no. PHY-9507695.

REFERENCES

- Aguirre, A. 1999a, ApJ, 512, L19
Aguirre, A. 1999b, ApJ, in press
Barger, A. J., Cowie, L. L., & Sanders, D. B. 1999a, ApJL, in press, astro-ph/9904126
Barger, A. J., Cowie, L. L., Smail, I., Ivison, R. J., Blain, A. W. & Kneib, J.-P. 1999b, AJ, in press; astro-ph/9903142
Bernstein, R. 1997, PhD thesis, Caltech
Blain, A. W. 1999, in Proc. of Photometric Redshift Meeting, OCIW, April 1999, preprint astro-ph/9906141
Blain, A. W., Kneib, J.-P., Ivison, R. J., & Smail, I. 1999, ApJ, 512, L87
Bond, J. R., Carr, B. J., & Hogan, C. J. 1991, ApJ, 367, 420
Bruzual, G., & Charlot, S. 1996, in preparation. The models are available from the anonymous ftp site gemini.tuc.noao.edu.
Draine, B. & Lee, H. 1984, ApJ, 285, 89
Eisenstein, D. J. 1997, ApJ, submitted, preprint astro-ph/9709054
Ferrara, A., Nath, B., Sethi, S. K. & Shchekinov, Y. 1999, MNRAS, 303, 301
Fixsen, D. J., Cheng, E. S., Gales, J. M., Mather, J. C., Shafer, R. A. & Wright, E. L. 1996, ApJ, 473, 576
Fixsen, D. J., Dwek, E., Mather, J. C., Bennett, C. L. & Shafer, R. A. 1998, ApJ, 508, 123
Gehrz, R. D. 1989, in "Interstellar Dust", Proc. of the 135th IAU Symposium, held in Santa Clara, California, 26-30 July, 1988, Eds. Louis J. Allamandola and A. G. G. M. Tielens, Kluwer Academic Publishers, Dordrecht, p.445
Guiderdoni, B., Hivon, E., Bouchet, F. R., & Maffei, B. 1998, MNRAS, 295, 877
Haiman, Z. & Knox, L. ApJL, submitted, preprint astro-ph/9906399
Haiman, Z. & Loeb, A. 1998, ApJ, 503, 505
Hauser, M. G., et al. 1998, ApJ, 508, 25
Hawkins, I. & Wright, E. 1988, ApJ, 324, 46
Hoyle, F. & Wickramasinghe, N. 1988, Ap&SS, 147, 245
Laor, A. & Draine, B. 1993, ApJ, 402, 441
Layzer, D. & Hively, R. 1973, ApJ, 179, 361
Loeb, A. & Haiman, Z. 1997, 490, 571
Madau, P. 1999, to appear in Physica Scripta, Proceedings of the Nobel Symposium, Particle Physics and the Universe (Enköping, Sweden, August 20-25, 1998), astro-ph/9902228
Madau, P., Pozzetti, L. & Dickinson, M. 1998, ApJ, 498, 106
Mathis, J., Rumpl, W. & Nordsieck, K. 1977, ApJ, 217, 425
Murthy, J., Henry, R. C. & Holberg, J. B. 1998, American Astronomical Society Meeting, 193, 6509
Pei, Y., Fall, M. & Hauser, M. 1998, ApJ, in press, astro-ph/9812182.
Perlmutter, S., et al. 1999, ApJ, 517, 565
Pozzetti, L., Madau, P., Zamorani, G., Ferguson, H. C. & Bruzual A., G. 1998, MNRAS, 298, 1133
Renzini, A. 1997, ApJ, 488, 35
Riess, A. G., et al. 1998, AJ, 116, 1009
Rowan-Robinson, M., Negroponte, J. & Silk, J. 1979, Nature, 281, 635
Stognienko, R., Henning, Th. & Ossenkopf, V. 1995, A&A, 296, 797
Vogele, M. 1997, ApJ, submitted, astro-ph/9711209
Wickramasinghe, N., Edmunds, M., Chitre, S., Narlikar, J., & Ramadurai, S. 1975, Ap&SS, 35, L9
Wickramasinghe, N. C. & Wallis, D. H. 1996, Ap&SS, 240, 157
Wollman, E. 1992, ApJ, 392, 80
Wright, E. L. 1981, ApJ, 250, 1
Wright, E. L. 1982, ApJ, 255, 401
Wright, E. L. 1987, ApJ, 320, 818

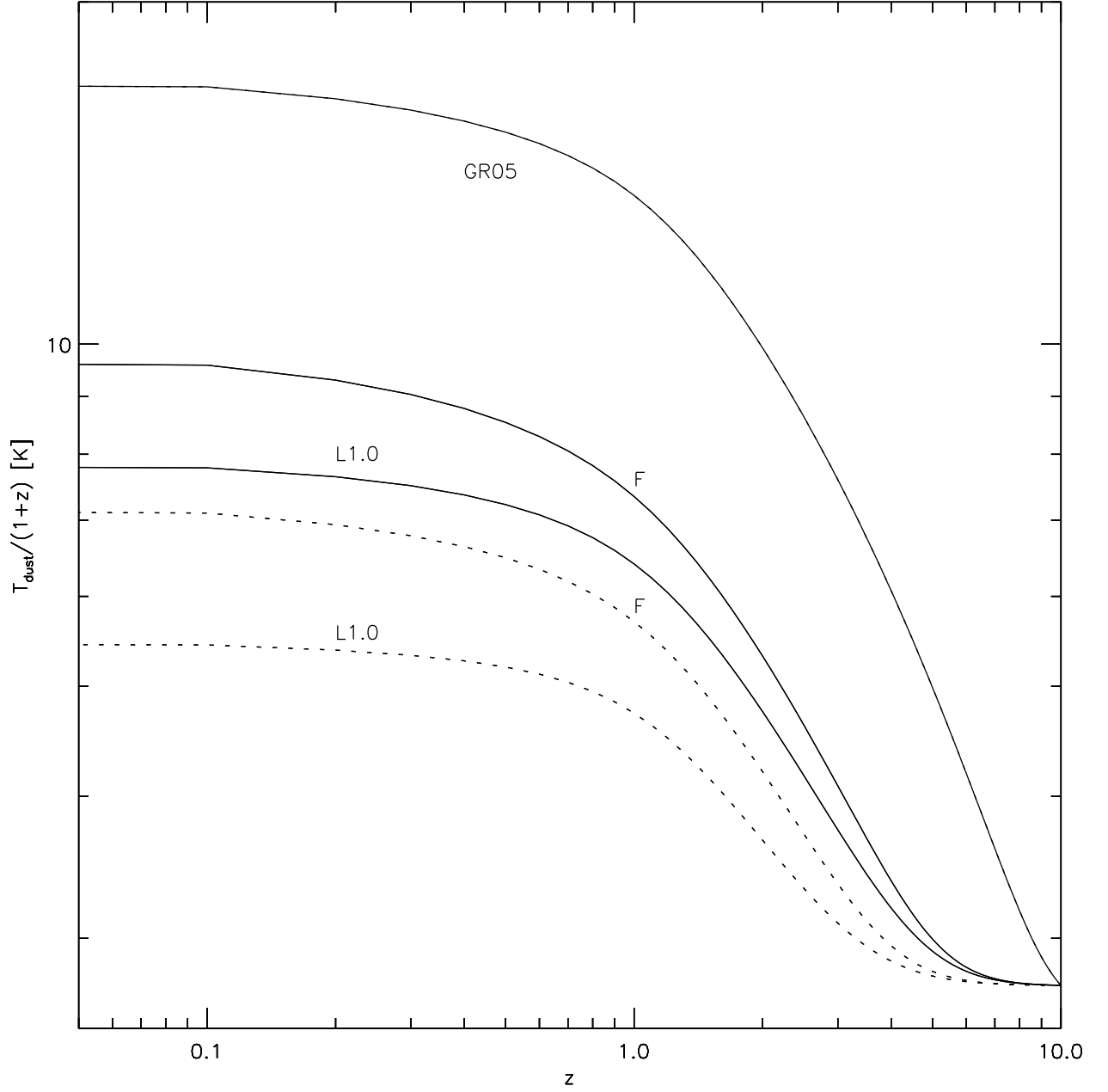


FIG. 1.— Evolution of dust temperature for silicate (dotted) and graphite (solid) grains in our fiducial model (F), a dust model with long-wavelength opacity $\propto \lambda^{-1}$ (L1.0) and a model with opacity that is constant for $\lambda < 0.5 \mu\text{m}$ and falls as λ^{-2} for longer λ (GR05). The dust temperatures in all other models fall in-between the two extreme models shown here.

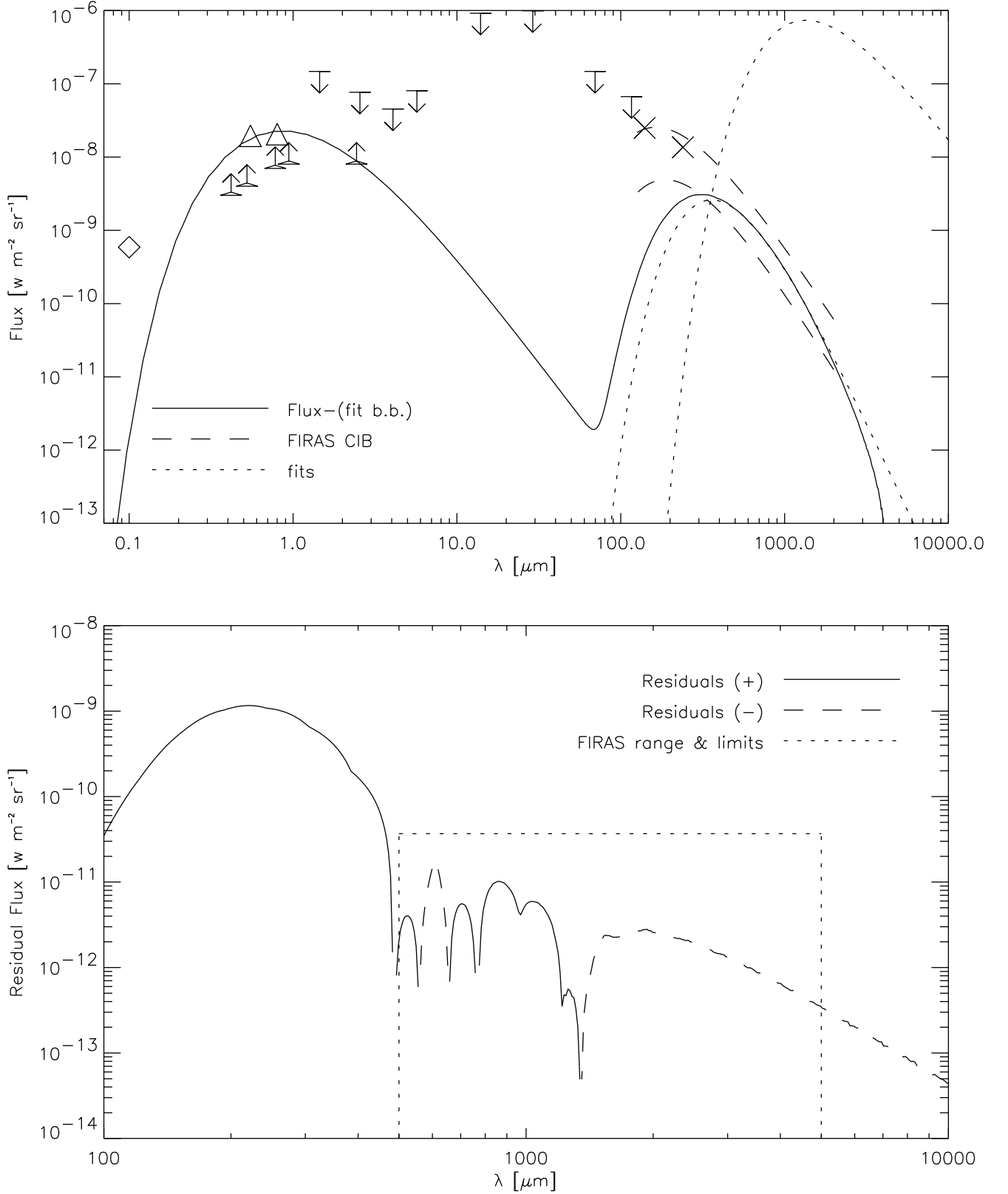


FIG. 2.— **Top:** Full $z = 0$ output spectrum (solid line) for our fiducial model, with the best-fit CMB (higher dotted line) subtracted. Also shown are the fitted $\nu^2 B_\nu$ component (lower dotted line), the FIRAS detected FIRB $\pm 1\sigma$ bounds (dashed), DIRBE FIRB detections (crosses) and upper limits (down arrows), the UVB detections (triangles) and HDF-derived lower limits (up arrows), and the Voyager FUV upper limit (diamond). **Bottom:** Spectrum with both CMB and $\nu^2 B_\nu$ component subtracted (solid and dashed lines). Vertical dotted lines represent the wavelength range over which the FIRAS distortion limit analysis was performed, the horizontal dotted line indicated the r.m.s. of the residuals in the FIRAS data. The features in the 500-5000 μm range indicate the level of numerical noise in our calculations.

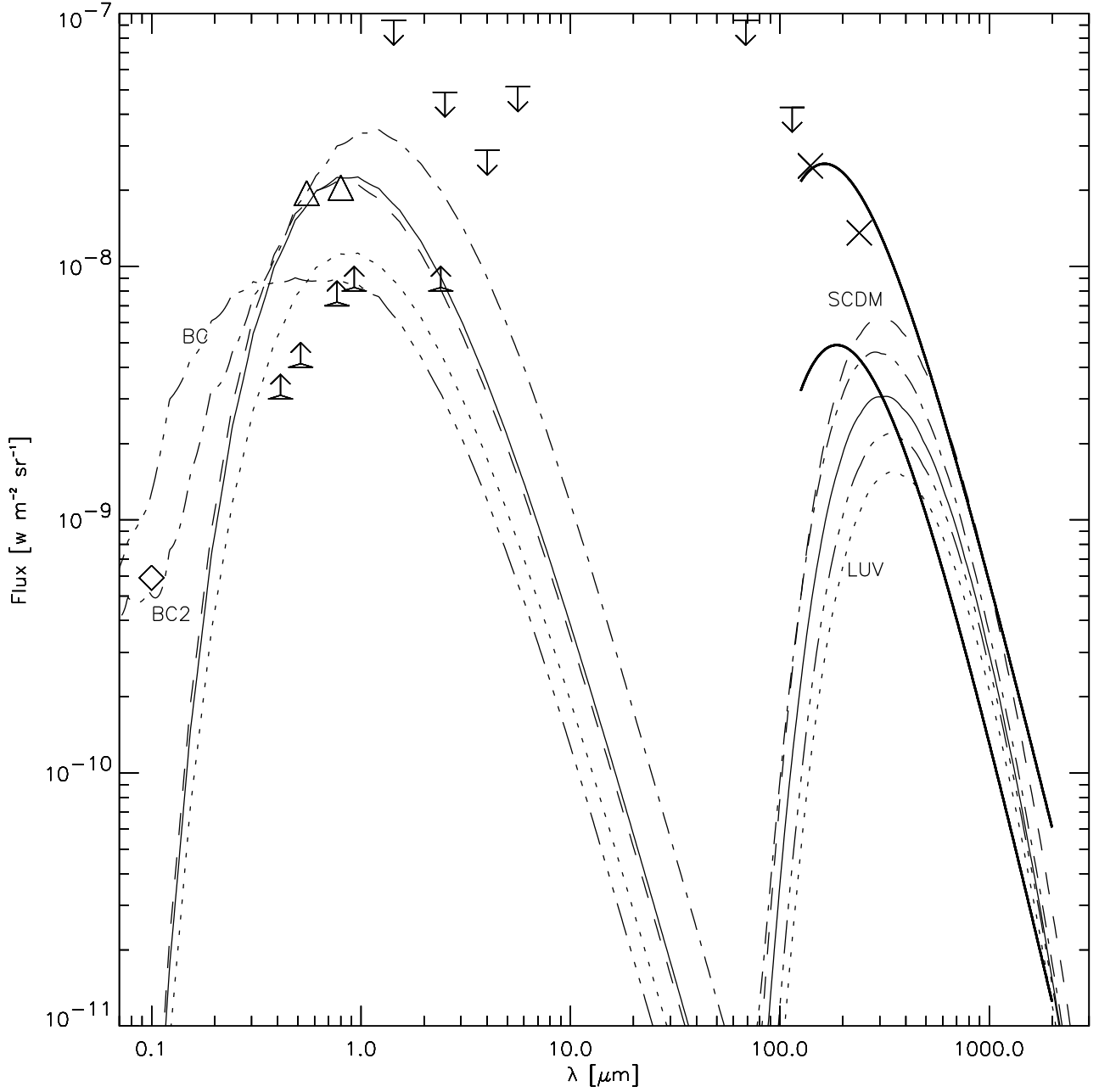


FIG. 3.— Output spectra for various models: A model using half the UVB normalization (LUV; dotted), an $\Omega = 1$ model (SCDM; dashed), and models with the Bruzual-Charlot spectral templates (BC; triple-dot-dashed), and reddened B-C templates (BC2; dot-dashed). The fiducial model is included (solid), as are UVB and FIRB limits as in Figure 2, with FIRAS FIRB detection limits in dark, solid. See text and Table 1 for details on models.

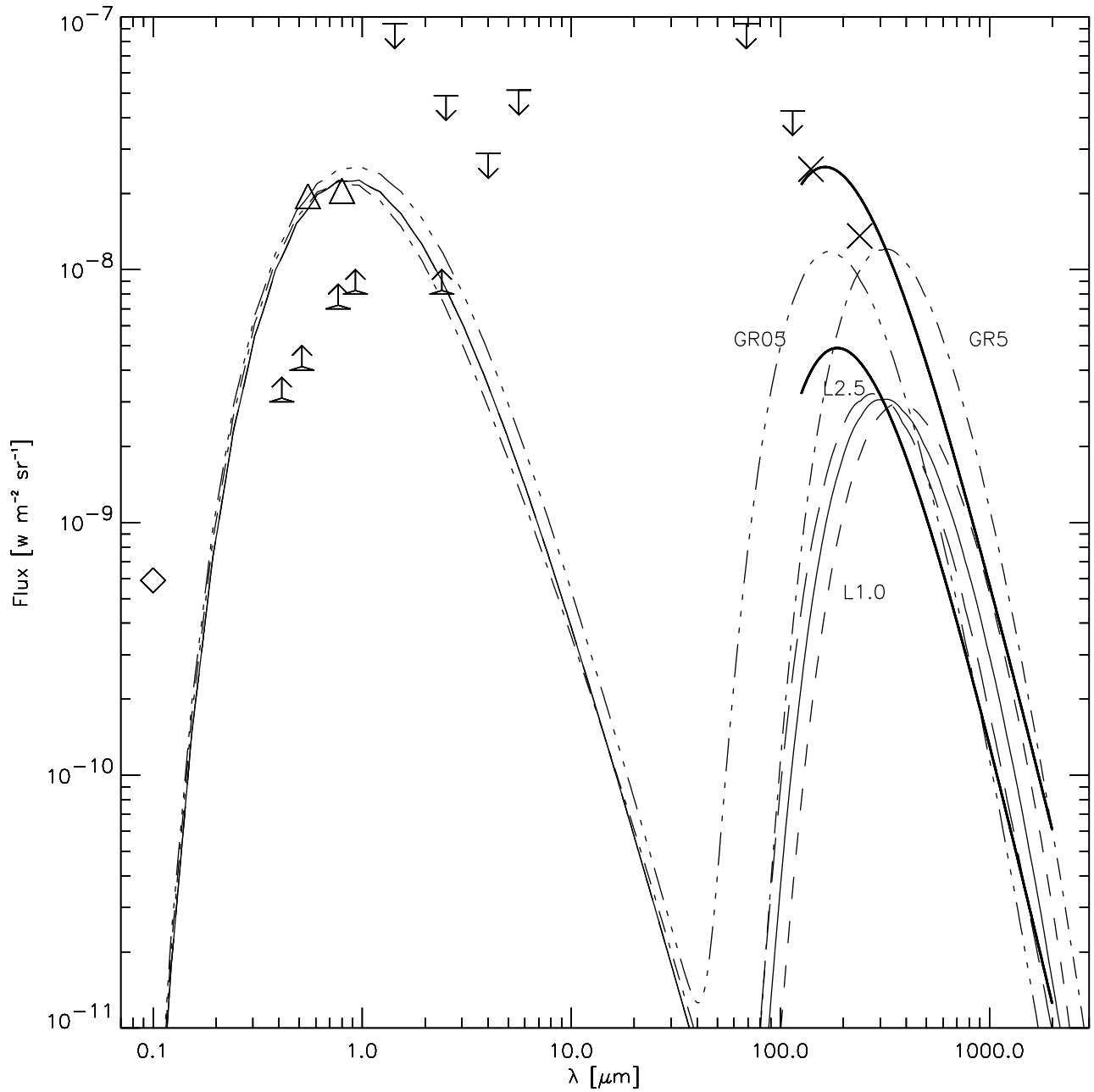


FIG. 4.— Output spectra for different dust models: A model with long-wavelength opacity $\propto \lambda^{-\alpha}$ for $\alpha = 1$ (L1.0; dashed) and $\alpha = 2.5$ (L2.5; long dashed), and models with dust which is grey out to λ_0 then falls as λ^{-2} , for $\lambda_0 = 0.5 \mu\text{m}$ (GR05; triple-dot-dashed) and for $\lambda_0 = 5 \mu\text{m}$ (GR5; dot-dashed). Again, the fiducial model is included (solid), as are UVB and FIRB limits as in Figure 2, with FIRAS FIRB detection limits in dark, solid. See text and Table 1 for details on models.